

# Analyzing Traffic Delay at Unmanaged Intersections

Changliu Liu and Mykel J. Kochenderfer

**Abstract**—At an unmanaged intersection, it is important to understand how much traffic delay may be caused as a result of microscopic vehicle interactions. Conventional traffic simulations that explicitly track these interactions are time-consuming. Prior work introduced an analytical traffic model for unmanaged intersections. The traffic delay at the intersection is modeled as an event-driven stochastic process, whose dynamics encode microscopic vehicle interactions. This paper studies the traffic delay in a two-lane intersection using the model. We perform rigorous analyses concerning the distribution of traffic delay under different scenarios. We then discuss the relationships between traffic delay and multiple factors such as traffic flow density, unevenness of traffic flows, temporal gaps between two consecutive vehicles, and the passing order.

## I. INTRODUCTION

Delay at intersections affect the capacity of a road network. There are many methods to analyze traffic delay at signalized intersections [1], [2], [3]. Such analyses are able to allow better traffic control to minimize delay. With the emergence of autonomous vehicles, there is a growing interest in leaving intersections unmanaged, allowing vehicles to resolve conflicts among themselves [4]. Unmanaged intersections can reduce infrastructure cost and allow for more flexible road network designs. Various vehicle policies have been proposed for distributed conflict resolution at unmanaged intersections [5], [6], [7].

It is important to understand how these microscopic policies affect the macroscopic transportation system. Toward the development of an efficient transportation system, we need to quantify the traffic delay generated during vehicle interactions at those intersections.

Delay at intersections is generally evaluated using microscopic traffic simulation [8]. Various evaluation platforms have been developed [9], including AIMSUN [10] and VISSIM [11]. However, it is time-consuming to obtain the micro-macro relationship by simulation. Only “point-wise” evaluation can be performed in the sense that a single parametric change in vehicle behaviors requires new simulations. In order to gain a deeper understanding of the micro-macro relationships, an analytical model is desirable.

In contrast with microscopic simulation models, macroscopic flow models [12] are analytical. Traffic is described by relations among aggregated values such as flow speed and density, without distinguishing its constituent parts. The major advantage of macroscopic flow models is their tractable mathematical structure with relatively few parameters to describe interactions among vehicles. However, it remains challenging to model intersections. Though intersections can be included

C. Liu and M. Kochenderfer are with the Department of Aeronautics and Astronautics, Stanford University, CA 94305 USA (e-mail: changliuliu, mykel@stanford.edu).

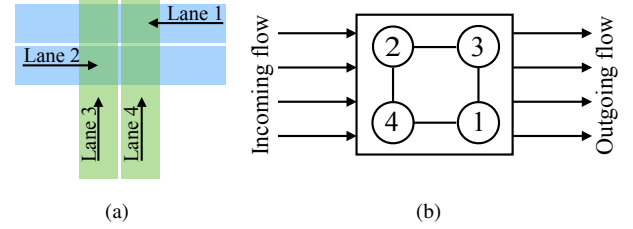


Fig. 1: Intersection scenario. (a) Road topology. (b) Conflict graph.

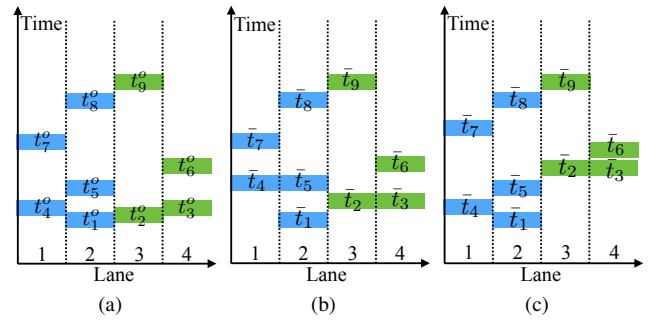


Fig. 2: The time of occupancy at the intersection. (a) The desired time of occupancy. (b) The actual time of occupancy under FIFO. (c) The actual time of occupancy under FO.

in the flow models as boundary constraints [13], [14], it is difficult to model policies other than the first-in-first-out (FIFO) policy. To consider a variety of policies, the vehicles need to be treated as particles that interact with one another, which has not been captured by existing flow models.

The authors introduced an analytical traffic model [15] to describe delays at unmanaged intersections. The model is event-driven, whose dynamics encodes equilibria resulting from microscopic vehicle interactions. It absorbs the advantages of both the microscopic simulation models and the macroscopic flow models. This paper performs detailed delay analysis at unmanaged intersections using the model. The following two components in a vehicle policy strongly influence the traffic delay: 1) determination of the passing order, and 2) the temporal gap between two consecutive vehicles to pass the intersection. We will illustrate how these two components as well as the distribution of incoming traffic flows affect delay.

The major contributions of this paper are:

- 1) Illustration of the usage of the analytical traffic model to obtain analytical distributions of delay.
- 2) Derivation of the analytical distribution of delay under two different classes of policies (i.e., two different passing orders) at a two-lane intersection;
- 3) Analysis of how traffic delay is affected by multiple factors at the two-lane intersection.

The remainder of the paper is organized as follows. Sec-

tion II reviews the analytical traffic model and illustrates how vehicle behaviors are encoded in the model. Section III derives the analytical distribution of delay under two different classes of policies. Section IV shows how the traffic delay is affected by multiple factors using the analytical distribution. Section V concludes the paper.

## II. TRAFFIC MODEL

This section reviews an event-driven stochastic model for traffic delay at intersections [15]. The following discussion considers an intersection with  $K$  incoming lanes. A conflict is where two incoming lanes intersect with each other. These relationships can be described in a conflict graph  $\mathcal{G}$  with the nodes being the incoming lanes and the links representing conflicts. Fig. 1a illustrates one possible road configuration with four incoming lanes, and Fig. 1b shows the resulting conflict graph.

### A. Microscopic Interactions

It is assumed that the vehicles at intersections have fixed paths. To respond to others during interactions, the vehicles only change their speed profiles to adjust the time to pass the intersection [16], [17]. This paper reduces the high dimensional speed profile for vehicle  $i$  to a single state  $t_i$ , which denotes the time for that vehicle to pass the center of the intersection. As the mapping from  $t_i$  to the speed profile is surjective, we can analyze interactions using  $t_i$ 's. The desired traffic-free time for vehicle  $i$  to pass the intersection is denoted  $t_i^o$ . The vehicles are indexed according to the desired passing time such that  $t_i^o \leq t_{i+1}^o$  for all  $i$ .

At time step  $k$ , vehicle  $i$  decides its passing time based on its desired time  $t_i^o$  and its observation of others' passing times at the last time step  $t_{-i}(k-1) := [t_1(k-1), \dots, t_{i-1}(k-1), t_{i+1}(k-1), \dots]$ . The policy of vehicle  $i$  is denoted

$$t_i(k) = f(t_i^o, t_{-i}(k-1)). \quad (1)$$

It is assumed that all vehicles use the same policy  $f$ .

### B. Equilibria

The equilibrium among the first  $i$  vehicles is denoted  $(\bar{t}_1^{(i)}, \dots, \bar{t}_i^{(i)})$ . In an equilibrium, no vehicle is willing to change the passing time before the arrival of the  $(i+1)$ th vehicle. Hence, the equilibrium is time-invariant, i.e.,

$$\bar{t}_j^{(i)} = f(t_j^o, \bar{t}_{-j}^{(i)}), \forall j \leq i. \quad (2)$$

It is assumed that an equilibrium can be achieved in negligible time. Hence, the system moves from the  $i$ th equilibrium to the  $(i+1)$ th equilibrium when the  $(i+1)$ th vehicle is included. The projected passing time for a vehicle may change from one equilibrium to another equilibrium, but will eventually converge to the actual passing time. The actual passing time  $\bar{t}_i$  for vehicle  $i$  is

$$\bar{t}_i = \lim_{j \rightarrow \infty} \bar{t}_i^{(j)}. \quad (3)$$

The problem of interest is to quantify the average delay

$$\bar{d} = \lim_{N \rightarrow \infty} \frac{1}{N} \sum_{i=1}^N (\bar{t}_i - t_i^o) = \lim_{N \rightarrow \infty} \frac{1}{N} \sum_{i=1}^N (\bar{t}_i^{(N)} - t_i^o). \quad (4)$$

Fig. 2a illustrates the desired time of occupancy for vehicles from the four lanes in Fig. 1a. The bars represent the moments that the intersection is occupied by vehicles, which is centered at  $t_i^o$ . According to the conflict graph, the scenario in Fig. 2a is infeasible as vehicles 1, 2, 3, and 4 cannot occupy the intersection at the same time. After some negotiation and adaptation among vehicles, the actual time of occupancy becomes as shown in Fig. 2b or Fig. 2c. For an unmanaged intersection, the actual time of occupancy depends on the policies that the vehicles adopt. Fig. 2b and Fig. 2c are different as they correspond to different policies, which will be discussed in detail in Section III-A. This paper quantifies the effectiveness of the policies based on the resulted average delay.

### C. Traffic Model at Intersections

For quantitative analysis, the traffic is modeled as an event-driven stochastic system with the state being the traffic delay and the input being the incoming traffic flow. The delay for lane  $k$  considering  $i$  vehicles is denoted  $T_i^k$ , which captures the difference between the passing time in the  $i$ th equilibrium and the traffic-free passing time of those vehicles, i.e.,

$$T_i^k = \max_{s_j=k, j \leq i} \bar{t}_j^{(i)} - t_i^o, \quad (5)$$

where  $s_j$  is the lane number of vehicle  $j$ . The input to the traffic model is the random arrival interval  $x_i = t_{i+1}^o - t_i^o$  between vehicle  $i+1$  and vehicle  $i$ , and the lane number  $s_{i+1}$  of vehicle  $i+1$ . Define  $\mathbf{T}_i := [T_i^1, \dots, T_i^K]^T$ . The dynamics of the traffic delay follow from

$$\mathbf{T}_{i+1} = \mathcal{F}(\mathbf{T}_i, x_i, s_{i+1}), \quad (6)$$

where the function  $\mathcal{F}$  depends on the policy  $f$  in (2) and the road topology defined by the conflict graph  $\mathcal{G}$  in Fig. 1b.

It is assumed that the desired passing time of the incoming traffic flow from lane  $k$  follows a Poisson distribution with parameter  $\lambda_k$ . The traffic flows from different lanes are independent of each other. Since the combination of multiple independent Poisson processes is a Poisson process [18], the incoming traffic from all lanes can be described as one Poisson process  $(t_1^o, t_2^o, \dots)$  with parameter  $\lambda = \sum_k \lambda_k$ . The probability density for  $x_i = x$  is  $p_x(x) = \lambda e^{-\lambda x}$ . The probability for  $s_{i+1} = k$  is  $P_s(k) = \frac{\lambda_k}{\lambda}$ .

Given (6), the conditional probability density of  $\mathbf{T}_{i+1}$  given  $\mathbf{T}_i$ ,  $x_i$  and  $s_{i+1}$  is

$$p_{\mathbf{T}_{i+1}}(\mathbf{t} \mid \mathbf{T}_i, x_i, s_{i+1}) = \delta(\mathbf{t} - \mathcal{F}(\mathbf{T}_i, x_i, s_{i+1})), \quad (7)$$

where  $\delta(\cdot)$  is the Dirac delta function. The total distribution is

$$\begin{aligned} & p_{\mathbf{T}_{i+1}}(\mathbf{t}) \\ &= \sum_k P_s(k) \int_x \int_{\boldsymbol{\tau}} p_{\mathbf{T}_{i+1}}(\mathbf{t} \mid \boldsymbol{\tau}, x, k) p_{\mathbf{T}_i}(\boldsymbol{\tau}) d\boldsymbol{\tau} p_x(x) dx \\ &= \sum_k P_s(k) \int_{\mathcal{F}(\boldsymbol{\tau}, x, k) = \mathbf{t}} \delta(0) p_{\mathbf{T}_i}(\boldsymbol{\tau}) p_x(x) d\boldsymbol{\tau} dx, \end{aligned} \quad (8)$$

which involves integration over a manifold. The cumulative probability of  $\mathbf{T}_i$  is denoted  $P_{\mathbf{T}_i}(\mathbf{t}) = \int_{-\infty}^{(t^1)^+} \cdots \int_{-\infty}^{(t^k)^+} p_{\mathbf{T}_i}(\tau^1, \dots, \tau^k) d\tau^1 \dots d\tau^k$  for  $\mathbf{t} = [t^1, \dots, t^k]$ .

In this paper, we investigate the steady state distribution  $p_{\mathbf{T}} := \lim_{i \rightarrow \infty} p_{\mathbf{T}_i}$ . Necessary conditions for the convergence of  $\lim_{i \rightarrow \infty} p_{\mathbf{T}_i}$  are provided in Section III. For simplicity, define the functional mapping  $\mathcal{M}$  as

$$\mathcal{M}(p)(\mathbf{t}) = \sum_k P_s(k) \int_{\mathcal{F}(\tau, x, k) = \mathbf{t}} \delta(0) p_x(x) p(\boldsymbol{\tau}) dx d\boldsymbol{\tau}. \quad (9)$$

The steady state distribution  $p_{\mathbf{T}}$  is a fixed point under  $\mathcal{M}$ .

#### D. Usage of the Model

Under the model, the distribution of vehicle delay can either be obtained through direct analysis or event-driven simulation.

1) *Theoretical Analysis*: The vehicle delay introduced by the  $(i+1)$ th vehicle is

$$d_{i+1} = \sum_{j \leq i} (\bar{t}_j^{(i+1)} - \bar{t}_j^{(i)}) + \bar{t}_{i+1}^{(i+1)} - t_{i+1}^*. \quad (10)$$

In the case that the introduction of a new vehicle only affects the last vehicle in other lanes (which is usually the case),

$$d_{i+1} = T_{i+1}^{s_{i+1}} + \sum_{k \neq s_{i+1}} (T_{i+1}^k - T_i^k + x_i). \quad (11)$$

Hence, to obtain an analytical steady state distribution of vehicle delay, we need to 1) obtain (6) from microscopic interactions models, then 2) solve the fixed point problem  $\mathcal{M}(p) = p$  for the steady state distribution  $p_{\mathbf{T}}$ , and finally 3) compute the steady state distribution of vehicle delay  $p_d$  from  $p_{\mathbf{T}}$  by (11). Section III illustrates the procedures for the derivation.

The relationship between  $\bar{d}$  in (4) and  $d_i$  in (10) is

$$\bar{d} = \lim_{N \rightarrow \infty} \frac{1}{N} \sum_i d_i. \quad (12)$$

According to the central limit theorem, the system is ergodic such that the average delay of all vehicles equals the expected delay introduced by a new vehicle (moving from one equilibrium to another equilibrium) in the steady state,

$$E(\bar{d}) = \lim_{i \rightarrow \infty} E(d_i). \quad (13)$$

2) *Event-Driven Simulation (EDS)*: The transition of the distribution from one equilibrium to another can also be simulated. Unlike conventional time-driven traffic simulation, we can perform event-driven simulation, which is more efficient. Many particles need to be generated for  $\mathbf{T}_0$ , each corresponding to one traffic scenario. Those particles are then propagated according to (6) by randomly sampling  $x_i$  and  $s_{i+1}$ . As the particles propagate, either the distribution diverges or we obtain the steady state distribution of delay.

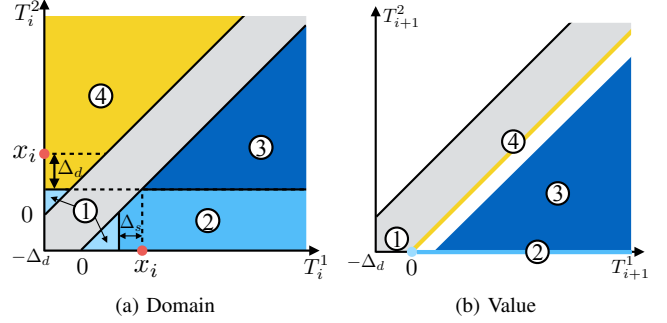


Fig. 3: Illustration of the mapping (6) under FIFO for  $s_{i+1} = 1$ .

### III. STEADY STATE DISTRIBUTION OF DELAY

This section derives the steady state distribution of delay under two classes of frequently used policies in a two-lane intersection using the method discussed in Section II-D1. The two policies are the first-in-first-out (FIFO) policy and the flexible order (FO) policy, which entail different passing orders. The required temporal gap between vehicles from different directions is denoted  $\Delta_d$ . The required temporal gap between vehicles from the same direction is denoted  $\Delta_s$ . The gap is affected by the following factors: vehicle speed, uncertainties in perception, and etc.

#### A. Vehicle Policies

The two classes of policies correspond to two ways to determine the passing order.

1) *FIFO*: The passing order is solely determined according to the arrival time (which is taken to be the desired passing time  $t_i^o$ ). The actual passing time for vehicle  $i$  should be after the actual passing times for all conflicting vehicles  $j$  such that  $j < i$ .<sup>1</sup> As the passing order is fixed, the actual passing time will not be affected by later vehicles, i.e.,  $\bar{t}_j = \bar{t}_j^{(i)} = \bar{t}_j^{(j)}$  for all  $i > j$ . For vehicle  $i$ ,

$$\bar{t}_i^{(i)} := \max\{t_i^o, \mathcal{D}_i, \mathcal{S}_i\}, \quad (14)$$

where  $\mathcal{D}_i$  is the earliest passing time considering vehicles from other lanes, and  $\mathcal{S}_i$  is the earliest passing time considering vehicles from the ego lane.

$$\mathcal{D}_i = \max_j (\bar{t}_j^{(i)} + \Delta_d) \text{ s.t. } j < i, (s_j, s_i) \in \mathcal{G}, \quad (15a)$$

$$\mathcal{S}_i = \max_j (\bar{t}_j^{(i)} + \Delta_s) \text{ s.t. } j < i, s_j = s_i. \quad (15b)$$

The effect of FIFO is illustrated in Fig. 2b.

2) *FO*: This strategy allows high priority vehicles to yield to low priority vehicles if low priority vehicles can arrive earlier. The passing order may change over time. At step  $i$ , let  $\bar{t}_i^{(i-1)} := \max\{t_i^o, \max_{j < i, s_j = s_i} (\bar{t}_j^{(i-1)} + \Delta_s)\}$  be the earliest possible time for vehicle  $i$  to pass considering its front vehicles in the ego lane. Sort the list  $(\bar{t}_1^{(i-1)}, \dots, \bar{t}_{i-1}^{(i-1)}, \bar{t}_i^{(i-1)})$

<sup>1</sup>Some authors define FIFO to be such that vehicle  $i$  should yield to vehicle  $j$  for all  $j < i$  no matter there is a conflict or not. The FIFO strategy presented in this paper is similar to the Maximum Progression Intersection Protocol (MP-IP) [6]. Nonetheless, there is no difference between the two in the two-lane scenario.

TABLE I: The mapping (6) under FIFO for  $s_{i+1} = 1$ .

Region	Condition	Value
1	$T_i^1 < x_i - \Delta_s$ $T_i^2 < x_i - \Delta_d$	$T_{i+1}^1 = 0$ $T_{i+1}^2 = -\Delta_d$
2	$T_i^1 \geq x_i - \Delta_s$ $T_i^2 < x_i - \Delta_d$ $T_i^2 < T_i^1$	$T_{i+1}^1 = T_i^1 + \Delta_s - x_i$ $T_{i+1}^2 = -\Delta_d$
3	$T_i^2 \geq x_i - \Delta_d$ $T_i^2 < T_i^1$	$T_{i+1}^1 = T_i^1 + \Delta_s - x_i$ $T_{i+1}^2 = T_i^2 - x_i$
4	$T_i^2 \geq x_i - \Delta_d$ $T_i^2 > T_i^1$	$T_{i+1}^1 = T_i^2 + \Delta_d - x_i$ $T_{i+1}^2 = T_i^2 - x_i$

in ascending order and record the ranking in  $Q : \mathbb{N} \rightarrow \mathbb{N}$ . If there is a tie, the vehicle with a smaller index is given a smaller  $Q$  value. For the first vehicle in  $Q$ , i.e., vehicle  $k = Q^{-1}(1)$ , the passing time is  $\bar{t}_k^{(i)} := \bar{t}_k^{(i-1)}$ . By induction, assuming that  $\bar{t}_j^{(i)}$  for  $Q(j) < Q(k)$  has been computed, then

$$\bar{t}_k^{(i)} := \max\{\bar{t}_k^{(i-1)}, \mathcal{D}_k^i, \mathcal{S}_k^i\}, \quad (16)$$

where

$$\mathcal{D}_k^i = \max_j(\bar{t}_j^{(i)} + \Delta_d) \text{ s.t. } Q(j) < Q(k), (s_j, s_k) \in \mathcal{G}, \quad (17a)$$

$$\mathcal{S}_k^i = \max_j(\bar{t}_j^{(i)} + \Delta_s) \text{ s.t. } Q(j) < Q(k), s_j = s_k. \quad (17b)$$

Under FO, the actual passing time may change over time. There is a distributed algorithm [7] to implement this policy where the vehicles do not necessarily need to compute the global passing order. The effect of FO is illustrated in Fig. 2c. Vehicles in the same direction tend to form groups and pass together. For a two-lane intersection, the passing order is changed if and only if the next vehicle can pass the intersection earlier than the last vehicle in the other lane.

### B. Case 1: Delay under FIFO

Following from (5) and (14), the dynamic equation (6) for FIFO can be computed, which is listed in Table I and illustrated in Fig. 3. Only the case for  $s_{i+1} = 1$  is shown. Define a conjugate operation  $(\cdot)^*$  as  $i^* := 3 - i$ . The case for  $s_{i+1} = 2$  can be obtained by taking the conjugate of all superscripts. In order to bound the domain from below, let  $T_i^j = \max\{T_i^j, -\Delta_d\}$  for all  $i$  and  $j \in \{1, 2\}$ . There are four smooth components in the mapping as illustrated in Fig. 3 and Table I. Region 1 corresponds to the case that there is enough gap in both lanes for vehicle  $i + 1$  to pass without any delay. Regions 2 and 3 correspond to the case that the last vehicle is from the ego lane and it causes delay for vehicle  $i + 1$ . Region 4 corresponds to the case that the last vehicle is from the other lane and it causes delay for vehicle  $i + 1$ .

Given the dynamic equation, the probability (8) can be computed. For simplicity, we only show the case for  $t^1 > t^2$ . The case for  $t^1 < t^2$  is symmetric. When  $t^2 = -\Delta_d$ ,  $P_{\mathbf{T}_{i+1}}(t^1, -\Delta_d) =$

$$P_s(1) \int_0^\infty P_{\mathbf{T}_i}(t^1 + x - \Delta_s, x - \Delta_d) p_x dx. \quad (18)$$

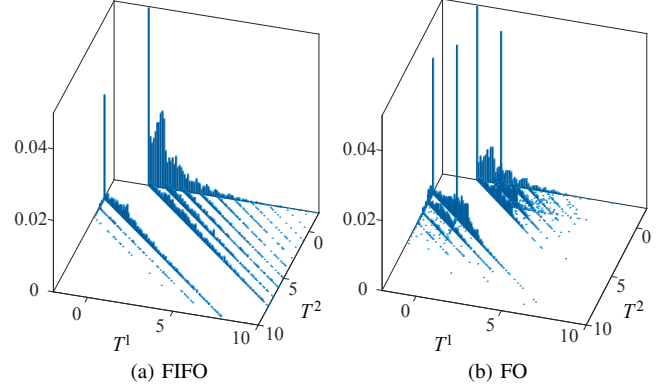


Fig. 4: The steady state distribution  $p_{\mathbf{T}}$  for  $\lambda_1 = 0.1 \text{ s}^{-1}$ ,  $\lambda_2 = 0.5 \text{ s}^{-1}$ ,  $\Delta_d = 2 \text{ s}$ , and  $\Delta_s = 1 \text{ s}$  from EDS with 10000 particles.

When  $t^1 = t^2 + \Delta_d$ ,  $p_{\mathbf{T}_{i+1}}(t^1, t^2) =$

$$P_s(1) \int_0^\infty \int_{-\Delta_d}^{t^2+x-\Delta_d} p_{\mathbf{T}_i}(\tau, t^2+x) d\tau p_x dx. \quad (19)$$

For  $t^1 > t^2 + \Delta_d > 0$ ,  $p_{\mathbf{T}_{i+1}}(t^1, t^2) =$

$$P_s(1) \int_0^\infty p_{\mathbf{T}_i}(t^1 - \Delta_s + x, t^2 + x) p_x dx. \quad (20)$$

**Proposition 1** (Necessary Condition for Convergence under FIFO). *The distributions  $\{p_{\mathbf{T}_i}\}_i$  converges for FIFO only if the following condition holds*

$$2\lambda_1\lambda_2\Delta_d + [\lambda_1^2 + \lambda_2^2]\Delta_s \leq \lambda. \quad (21)$$

*Proof.* The convergence of the distribution implies the convergence of the expected delay. Hence, the minimum average departure interval between two consecutive vehicles should be smaller than the average arrival interval. For two consecutive vehicles, the probability that they are from the same lane is  $P_s(1)^2 + P_s(2)^2$ , and the probability that they are from different lanes is  $2P_s(1)P_s(2)$ . Hence, the minimum average departure interval is  $2P_s(1)P_s(2)\Delta_d + [P_s(1)^2 + P_s(2)^2]\Delta_s$ . The average arrival interval is  $\frac{1}{\lambda}$ . The convergence of the distribution implies

$$2P_s(1)P_s(2)\Delta_d + [P_s(1)^2 + P_s(2)^2]\Delta_s \leq \frac{1}{\lambda}. \quad (22)$$

Condition (21) can be obtained by rearranging (22).  $\square$

The proof of the sufficiency of (21) is left as future work. In the following discussion, we investigate the steady state distribution  $p_{\mathbf{T}} = \mathcal{M}(p_{\mathbf{T}})$  for  $\Delta_s > 0$  and  $\Delta_s = 0$ .

**Proposition 2** (Steady State Distribution for  $\Delta_s > 0$  under FIFO). *When  $\Delta_s > 0$ , for  $t > -\Delta_d$  and  $\Gamma > \Delta_d$ , the following equalities hold,*

$$p_{\mathbf{T}}(t + \Gamma, t) = C_n^1 \int_0^\infty p_{\mathbf{T}}(\hat{t} + \gamma, \hat{t}) e^{-\lambda z} z^{n-1} dz, \quad (23a)$$

$$p_{\mathbf{T}}(t, t + \Gamma) = C_n^2 \int_0^\infty p_{\mathbf{T}}(\hat{t}, \hat{t} + \gamma) e^{-\lambda z} z^{n-1} dz, \quad (23b)$$

where  $n$  is the maximum integer such that  $\gamma := \Gamma - n\Delta_s \in (\Delta_d - \Delta_s, \Delta_d]$ ,  $C_n^i = \frac{\lambda^n}{(n-1)!}$ , and  $\hat{t} = t + z$ . Moreover,

$p_{\mathbf{T}}(t^1, t^2) = 0$  if  $\min\{t^1, t^2\} > -\Delta_d$  and  $|t^1 - t^2| \neq \Delta_d + n\Delta_s$  for any  $n \in \mathbb{N}$ .

*Proof.* Since (23a) and (23b) are symmetric, we will only show the derivation for (23a) for simplicity. By (20),

$$\begin{aligned} & p_{\mathbf{T}}(t + n\Delta_s + \gamma, t) \\ &= P_s(1) \int_0^\infty p_{\mathbf{T}}(t + (n-1)\Delta_s + \gamma + x_1, t + x_1) p_{\mathbf{x}} dx_1 \end{aligned}$$

By induction on  $n$ ,

$$p_{\mathbf{T}}(t + \Gamma, t) = P_s(1)^n \int_{\mathbf{x} \geq 0} p_{\mathbf{T}}(t + z + \gamma, t + z) p_{\mathbf{x}} d\mathbf{x},$$

where  $\mathbf{x} = [x_1, x_2, \dots, x_n]$ ,  $z = \sum_{k=1}^n x_k$ , and  $p_{\mathbf{x}}(\mathbf{x}) = \lambda^n e^{-\lambda z}$ . By change of variable from  $\mathbf{x}$  to  $[z, x_2, \dots, x_n]$ ,

$$p_{\mathbf{T}}(t + \Gamma, t) = \lambda_1^n \int_0^\infty V(z, n-1) p_{\mathbf{T}}(t + z + \gamma, t + z) e^{-\lambda z} dz,$$

where  $V(z, n-1) = \frac{1}{(n-1)!} z^{n-1}$  is the volume of an  $(n-1)$ -dimensional cone with depth  $z$ .<sup>2</sup> Hence, (23a) is verified.

If  $\gamma \in (\Delta_d - \Delta_s, \Delta_d)$ , by definition,  $p_{\mathbf{T}}(t + \gamma, t) = 0$ . Then  $p_{\mathbf{T}}(t + n\Delta_s + \gamma, t) = 0$  for any  $n \in \mathbb{N}$  according to (23a). Similarly,  $p_{\mathbf{T}}(t, t + n\Delta_s + \gamma) = 0$  for any  $n \in \mathbb{N}$ . Hence,  $p_{\mathbf{T}}(t^1, t^2) = 0$  if  $\min\{t^1, t^2\} > -\Delta_d$  and  $|t^1 - t^2| \neq \Delta_d + n\Delta_s$  for any  $n \in \mathbb{N}$ .  $\square$

Proposition 2 implies a unique ‘‘zebra’’ pattern of the steady state lane delay. This pattern is also observed in EDS shown in Fig. 4a. The exact solution of  $p_{\mathbf{T}}$  for  $\Delta_s > 0$  is left as future work. In the following discussion, we derive the case for  $\Delta_s = 0$ . The assumption that  $\Delta_s = 0$  is valid when the traffic density is low. Lemma 3 is useful in the derivation of the steady state delay.

**Lemma 3 (Zero Function).** *For any norm-bounded  $L_1$  function  $f$ , if  $f(t) = a \int_0^\infty f(t+x) e^{-\lambda x} dx$  for all  $t$  and  $\lambda \leq a > 0$ , then  $f \equiv 0$ .*

*Proof.* Multiply  $e^{-\lambda t}$  on both sides, then

$$e^{-\lambda t} f(t) = a \int_0^\infty f(t+x) e^{-\lambda(x+t)} dx = a \int_t^\infty f(x) e^{-\lambda x} dx.$$

Take derivative with respect to  $t$  on both sides, then

$$e^{-\lambda t} f'(t) - \lambda e^{-\lambda t} f(t) = -a f(t) e^{-\lambda t},$$

which implies that  $f'(t) = (\lambda - a)f(t)$  and  $f(t) = C e^{(\lambda-a)t}$  for some constant  $C$ . However, since  $\lambda - a \geq 0$ ,  $f$  cannot be norm bounded if  $C \neq 0$ . Hence,  $f \equiv 0$ .  $\square$

In the following discussion, we derive the steady state distribution of delay for  $\Delta_s = 0$ . Proposition 4 shows that when  $\Delta_s = 0$ , the probability density is non trivial only at  $p_{\mathbf{T}}(t, t - \Delta_d)$  or  $p_{\mathbf{T}}(t - \Delta_d, t)$  for  $t \geq 0$ . Hence, we define

$$g_1(t) := p_{\mathbf{T}}(t, t - \Delta_d), g_2(t) := p_{\mathbf{T}}(t - \Delta_d, t). \quad (24)$$

The function  $g_i$  for  $i \in \{1, 2\}$  contains both finite component and delta component, denoted  $\tilde{g}_i$  and  $\hat{g}_i$  respectively such that

<sup>2</sup> $V(z, n-1) = \int_0^z \int_0^{z-x_2} \dots \int_0^{z-x_2-\dots-x_{n-1}} dx_n \dots dx_3 dx_2.$

$g_i(t) = \tilde{g}_i(t) + \hat{g}_i(t)\delta(t)$ . Moreover, for  $i \in \{1, 2\}$ , define the probability function  $G_i$ , value  $\mathcal{M}_i$  and value  $\mathcal{I}_i$  as

$$G_i(t) := \int_0^t g_i(\tau) d\tau, \quad (25a)$$

$$\mathcal{M}_i := \int_0^\infty g_i(x) dx, \quad (25b)$$

$$\mathcal{I}_i := \int_0^\infty g_i(x) e^{-\lambda x} dx. \quad (25c)$$

Value  $\mathcal{M}_i$  is the probability that lane  $i$  has larger delay.

**Proposition 4 (Steady State Distribution for  $\Delta_s = 0$  under FIFO).** *When  $\Delta_s = 0$ ,  $p_{\mathbf{T}}(t^1, t^2) = 0$  if  $|t^1 - t^2| \neq \Delta_d$ . For  $i \in \{1, 2\}$ , the following equations hold*

$$G_i(t) = \hat{g}_i(0) e^{\lambda_i^* t}, \text{ for } t \in [0, \Delta_d], \quad (26)$$

$$\hat{g}_i(t) = \begin{cases} \frac{\lambda_i}{\lambda} [\mathcal{I}_i + e^{-\lambda \Delta_d} \mathcal{I}_{i^*}] & t = 0 \\ 0 & t \neq 0 \end{cases}, \quad (27)$$

$$\lambda_i \hat{g}_i^*(0) = \tilde{g}_i(\Delta_d^-) - \tilde{g}_i(\Delta_d^+), \quad (28)$$

$$\mathcal{M}_i = \frac{\lambda_i}{\lambda}. \quad (29)$$

Moreover, when  $t$  is sufficiently large,

$$\mathcal{M}_i - G_i(t) \propto e^{-at}, \quad (30)$$

where  $a < 0$  is the solution of the following equation

$$(a - \lambda_1)(a - \lambda_2) - \lambda_1 e^{-a\Delta_d} \lambda_2 e^{-a\Delta_d} = 0. \quad (31)$$

*Proof.* We first show that  $p_{\mathbf{T}}(t^1, t^2) = 0$  if  $|t^1 - t^2| \neq \Delta_d$ . There are two cases:  $\min\{t^1, t^2\} > -\Delta_d$  or  $\min\{t^1, t^2\} = -\Delta_d$ . Consider  $\Gamma > \Delta_d$  and  $t > -\Delta_d$ . According to (20),

$$p_{\mathbf{T}}(t + \Gamma, t) = \lambda_1 \int_0^\infty p_{\mathbf{T}}(t + x + \Gamma, t + x) e^{-\lambda x} dx. \quad (32)$$

By Lemma 3, (32) implies  $p_{\mathbf{T}}(t + \Gamma, t) \equiv 0$  for all  $t > -\Delta_d$ . Similarly,  $p_{\mathbf{T}}(t, t + \Gamma) \equiv 0$  for all  $t > -\Delta_d$ . Moreover, for  $t > 0$ , according to (18),

$$p_{\mathbf{T}}(t, -\Delta_d) = \lambda_1 \int_0^\infty p_{\mathbf{T}}(t + x, -\Delta_d) e^{-\lambda x} dx. \quad (33)$$

By Lemma 3, (33) implies  $p_{\mathbf{T}}(t, -\Delta_d) \equiv 0$  for  $t > 0$ . Similarly,  $p_{\mathbf{T}}(-\Delta_d, t) \equiv 0$  for  $t > 0$ . Hence, the claim is verified.

Now we compute the steady state distribution  $g_i$ . In either  $g_1$  or  $g_2$ , there is only one point mass at 0 by (18) to (20). According to (18),

$$\begin{aligned} & \hat{g}_i(0) \\ &= \lambda_i \int_0^\infty \left[ \int_0^x g_i(t) dt + \int_0^{x-\Delta_d} g_{i^*}(t) dt \right] e^{-\lambda x} dx \\ &= \lambda_i \int_0^\infty \left[ \int_t^\infty e^{-\lambda x} dx g_i + \int_0^\infty \int_{t+\Delta_d}^\infty e^{-\lambda x} dx g_{i^*} \right] dt \\ &= \frac{\lambda_i}{\lambda} \left[ \int_0^\infty g_i(t) e^{-\lambda t} dt + \int_0^\infty g_{i^*}(t) e^{-\lambda(t+\Delta_d)} dt \right], \quad (34) \end{aligned}$$

where the second equality is obtained by changing the order of integration. By definition (25c), (34) implies (27).



According to (19) and (20), for  $t > 0$ ,

$$\tilde{g}_i(t) = \lambda_i \int_0^\infty [g_i(t+x) + g_{i^*}(t+x-\Delta_d)] e^{-\lambda x} dx, \quad (35)$$

which implies that  $\tilde{g}_i$  is continuous except at  $\Delta_d$ . The discontinuity at  $\Delta_d$  is caused by the point mass  $\hat{g}_{i^*}(0)$ . By (35), the claim in (28) is verified. By multiplying  $e^{-\lambda t}$  on both sides of (35) and then taking derivatives similar to the proof in Lemma 3, we obtain the following differential equation

$$\tilde{g}'_i(t) = \lambda_{i^*} \tilde{g}_i(t) - \lambda_i \tilde{g}_{i^*}(t - \Delta_d). \quad (36)$$

For  $t \in (0, \Delta_d)$ , since  $\tilde{g}_{i^*}(t - \Delta_d) = 0$ , (36) implies that there exists  $c_i \in \mathbb{R}^+$  such that

$$\tilde{g}_i(t) = c_i e^{\lambda_{i^*} t}. \quad (37)$$

Plugging (37) back to (35), the constant  $c_i$  can be computed,

$$c_i = \lambda_i [\mathcal{I}_i - \hat{g}_i(0) + e^{-\lambda \Delta_d} \mathcal{I}_{i^*}] = \lambda_{i^*} \hat{g}_i(0). \quad (38)$$

Then (26) is verified by integrating (37). Moreover, it is easy to verify that  $\mathcal{M}_i = P_s(i) = \frac{\lambda_i}{\lambda}$ . Hence, (26) to (29) are all verified.

The characteristic equation [19] of the delay differential equation (36) for  $i \in \{1, 2\}$  satisfies

$$\det \left( aI_2 - \begin{bmatrix} \lambda_2 & 0 \\ 0 & \lambda_1 \end{bmatrix} + e^{-a\Delta_d} \begin{bmatrix} 0 & \lambda_1 \\ \lambda_2 & 0 \end{bmatrix} \right) = 0, \quad (39)$$

which is equivalent to the nonlinear eigenproblem (31). There are three possible solutions with  $a = 0$ ,  $a > 0$ , and  $a < 0$ , respectively. Since  $\lim_{t \rightarrow \infty} g_i(t) = 0$ , we can only take the solution  $a < 0$ . When  $t \rightarrow \infty$ ,  $g_i(t)$  is proportional to  $e^{at}$ . Then (30) is verified.  $\square$

To compute the exact solution of the distribution, the delay differential equation (DDE) (36) needs to be solved. To solve the DDE, we need to compute the expression of  $G_i(t)$  for  $t \in ((n-1)\Delta_d, n\Delta_d]$  consecutively for all  $n$  considering the boundary constraints (26) to (29). However, as there are infinitely many segments, the complexity of the problem grows quickly. In this paper, we approximate the distribution for  $t > \Delta_d$  using (30). By incorporating (26) and (29), the approximated distribution is

$$G_i(t) = \begin{cases} \hat{g}_i(0) e^{\lambda_{i^*} t} & t \leq \Delta_d \\ \frac{\lambda_i}{\lambda} (1 - e^{a(t-\Delta_d)}) + G_i(\Delta_d) e^{a(t-\Delta_d)} & t > \Delta_d \end{cases}. \quad (40)$$

There is only one unknown parameter  $\hat{g}_i(0)$ , which can be solved by the remaining equations in Proposition 4. However, the approximated distribution (40) is not simultaneously compatible with (27) and (28). We need to relax either condition. Equation (27) is a global condition as it is related to the integral of the distribution. Equation (28) is a local condition as it concerns the discontinuous point of the probability density.

**Remark 1** (Approximation 1). *In the first approximation, the local condition (28) is relaxed. Then  $\hat{g}_i(0)$  is obtained by solving (27) and (40),*

$$\hat{g}_i(0) = \frac{a\lambda_i y ((\lambda_i - a)\lambda_i(y^2 - 1) + (a - \lambda)y_i [\lambda_{i^*} + \lambda_i y])}{B_i}, \quad (41)$$

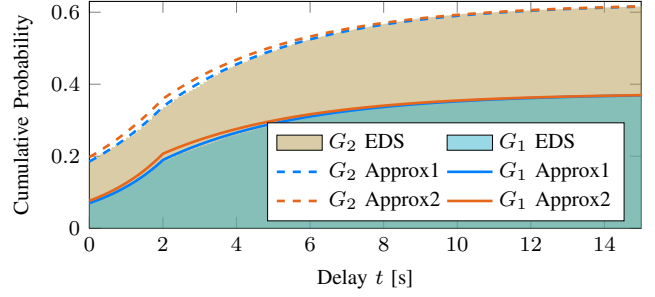


Fig. 5: Steady state traffic delay under FIFO.  $\lambda_1 = 0.3 \text{ s}^{-1}$ ,  $\lambda_2 = 0.5 \text{ s}^{-1}$ ,  $\Delta_d = 2 \text{ s}$ , and  $\Delta_s = 0 \text{ s}$ .

where  $y := e^{-\lambda \Delta_d}$ ,  $y_i := e^{-\lambda_i \Delta_d}$ , and

$$B_i = \lambda^2 (a^2 y (y - y_i) (1 - y_i) + a(a - \lambda) y_i + (a - \lambda_i) \lambda y^2 (y_i - 1) + (2a - \lambda) \lambda y y_i (1 - y_i) + (a - \lambda) \lambda_i y y_i^2 + \lambda_i \lambda_{i^*} y_i + \lambda_i^2 y^2 y_i - a \lambda_i y^2). \quad (42)$$

**Remark 2** (Approximation 2). *In the second approximation, we relax the global condition (27). Then  $\hat{g}_i(0)$  is obtained by solving (28) and (40),*

$$\hat{g}_i(0) = \frac{a\lambda_i y e^{a\Delta_d} (\lambda_i + \lambda_{i^*} y_i - a e^{a\Delta_d})}{\lambda (a\lambda e^{a\Delta_d} - a^2 e^{2a\Delta_d} + \lambda_i \lambda_{i^*} (y - 1))}. \quad (43)$$

The accuracy of the two approximations against the steady state distribution obtained from EDS with 10000 particles is shown in Fig. 5. Though both underestimate the delay, (41) provides a better approximation because it preserves the global property. In the following discussion and analysis, we use the first approximation.

**Corollary 5** (Approximated Steady State Vehicle Delay). *When  $\Delta_s = 0$ , under the approximation (40), the steady state vehicle delay has the distribution*

$$P_d(t) = \begin{cases} \hat{g}_1(0) e^{\lambda_2 t} + \hat{g}_2(0) e^{\lambda_1 t} & t \leq \Delta_d \\ 1 - e^{a(t-\Delta_d)} + P_d(\Delta_d) e^{a(t-\Delta_d)} & t > \Delta_d \end{cases}, \quad (44)$$

with expected delay

$$E(d) = \hat{g}_1(0) \mathcal{E}(\lambda_2) + \hat{g}_2(0) \mathcal{E}(\lambda_1) - \frac{(a\Delta_d - 1)(P_d(\Delta_d) - 1)}{a}, \quad (45)$$

where

$$\mathcal{E}(\lambda_i) = \frac{1 + e^{\Delta_d \lambda_i} (\Delta_d \lambda_i - 1)}{\lambda_i}. \quad (46)$$

*Proof.* By (11), the vehicle delay in the steady state satisfies that  $P_d(t) = G_1(t) + G_2(t)$ . So (44) follows from (40). The expected delay satisfies  $E(d) = \int_0^\infty t dP_d(t)$ . Let  $\mathcal{E}(\lambda_i) := \int_0^{\Delta_d} t d e^{\lambda_i t}$ . Then (45) and (46) follow.  $\square$

### C. Case 2: Delay under FO

Following from (5) and (16), the dynamic equation (6) for FO can be computed, which is listed in Table II and illustrated in Fig. 6 for  $s_{i+1} = 1$ . There are eight smooth components in the mapping. Regions 1 to 4 are the same as in the FIFO case. Vehicle  $i + 1$  is the last one to pass the intersection. Regions 5 to 8 correspond to the case that vehicle  $i + 1$  passes the intersection before the last vehicle in the other lane. In

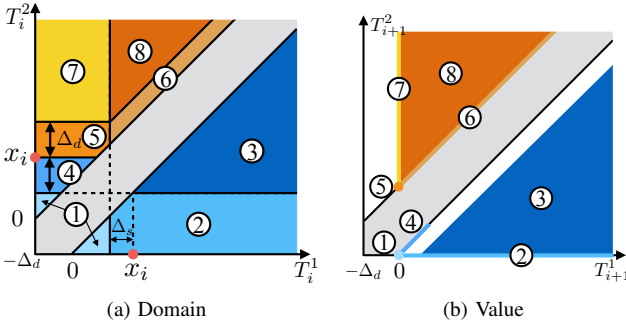


Fig. 6: Illustration of the mapping (6) under FO for  $s_{i+1} = 1$ .

regions 5 and 7, vehicle  $i + 1$  arrives earlier than the last vehicle in the other lane and there is enough gap in the ego lane. Hence, vehicle  $i + 1$  passes without delay, but the last vehicle in the other lane yields (with delay in region 5, without delay in region 7). Regions 6 and 8 correspond to the case that vehicle  $i + 1$  is delayed by the last vehicle in the ego lane but can still go before the last vehicle in the other lane. Delay is caused in the other lane in region 6.

Given the dynamic equation, the probability (8) can be computed. The distribution obtained from EDS with the same condition as in the FIFO case is shown in Fig. 4b. FO generates smaller delay as compared to FIFO, but FO no longer has the “zebra” pattern shown in FIFO.

In the following discussion, we discuss the necessary condition for convergence under FO and derive the exact steady state distribution of delay for  $\Delta_s = 0$ . The distribution for  $\Delta_s > 0$  is left as future work. Recall the definitions  $y = e^{-\lambda\Delta_d}$  and  $y_i = e^{-\lambda_i\Delta_d}$  for  $i \in \{1, 2\}$ .

**Proposition 6** (Necessary Condition for Convergence under FO). *The distributions  $\{p_{\mathbf{T}_i}\}_i$  converges for FO only if the following condition holds*

$$\lambda_1 \lambda_2 (y_1 + y_2) \Delta_d + [\lambda_1^2 + \lambda_2^2 + \lambda_1 \lambda_2 (2 - y_1 - y_2)] \Delta_s \leq \lambda. \quad (47)$$

*Proof.* Similar to the discussion in Proposition 1, the minimum average departure interval between two consecutive vehicles should be smaller than the average arrival interval. As FO adjusts the passing order, vehicles from the same lane may be grouped and pass the intersection together. For two vehicles consecutively leaving the intersection, they go to different lanes only if the following two conditions holds: 1) they come from different lanes and 2) the last vehicle in the two has a temporal gap greater than  $\Delta_d$  with its front vehicle. Hence, the probability that two departure vehicles are from different lanes is  $P_s(1)P_s(2)(e^{-\lambda_1\Delta_d} + e^{-\lambda_2\Delta_d})$ , which is smaller than  $2P_s(1)P_s(2)$ . The minimum average departure interval is  $P_s(1)P_s(2)(y_1 + y_2)\Delta_d + [P_s(1)^2 + P_s(2)^2 + P_s(1)P_s(2)(2 - y_1 - y_2)]\Delta_s$ . The average arrival interval is  $\frac{1}{\lambda}$ . Condition (21) can be obtained by requiring the minimum departure interval be smaller than the arrival interval.  $\square$

TABLE II: The mapping (6) under FO for  $s_{i+1} = 1$ .

	Domain	Value
1	$T_i^1 < x_i - \Delta_s$ $T_i^2 < x_i - \Delta_d$	$T_{i+1}^1 = 0$ $T_{i+1}^2 = -\Delta_d$
2	$T_i^1 \geq x_i - \Delta_s$ $T_i^2 < x_i - \Delta_d$ $T_i^2 < T_i^1$	$T_{i+1}^1 = T_i^1 + \Delta_s - x_i$ $T_{i+1}^2 = -\Delta_d$
3	$T_i^2 \geq x_i - \Delta_d$ $T_i^2 < T_i^1$	$T_{i+1}^1 = T_i^1 + \Delta_s - x_i$ $T_{i+1}^2 = T_i^2 - x_i$
4	$T_i^2 \in [x_i - \Delta_d, x_i)$ $T_i^2 > T_i^1$	$T_{i+1}^1 = T_i^2 + \Delta_d - x_i$ $T_{i+1}^2 = T_i^2 - x_i$
5	$T_i^2 \in [x_i, x_i + \Delta_d)$ $T_i^1 < x_i - \Delta_s$	$T_{i+1}^1 = 0$ $T_{i+1}^2 = \Delta_d$
6	$T_i^2 - T_i^1 \in [\Delta_d, \Delta_d + \Delta_s]$ $T_i^1 \geq x_i - \Delta_s$	$T_{i+1}^1 = T_i^1 - x_i + \Delta_s$ $T_{i+1}^2 = T_i^1 - x_i + \Delta_s + \Delta_d$
7	$T_i^1 < x_i - \Delta_s$ $T_i^2 \geq x_i + \Delta_d$	$T_{i+1}^1 = 0$ $T_{i+1}^2 = T_i^2 - x_i$
8	$T_i^2 - T_i^1 > x_i + \Delta_d + \Delta_s$ $T_i^1 \geq x_i - \Delta_s$	$T_{i+1}^1 = T_i^1 - x_i + \Delta_s$ $T_{i+1}^2 = T_i^2 - x_i$

**Proposition 7** (Steady State Distribution for  $\Delta_s = 0$  under FO). *If  $\Delta_s = 0$ , then  $p_{\mathbf{T}}(t^1, t^2) = 0$  if  $|t^1 - t^2| \neq -\Delta_d$  or  $t^1 + t^2 > \Delta_d$ . Moreover, for  $i \in \{1, 2\}$ ,*

$$G_i(t) = \begin{cases} \frac{c_i}{\lambda_{i^*}} e^{\lambda_{i^*} t} & t \in [0, \Delta_d) \\ \mathcal{M}_i & t \geq \Delta_d \end{cases}, \quad (48)$$

$$\mathcal{M}_i = \frac{\lambda_i}{\lambda}, \quad (49)$$

$$c_i = \frac{\lambda_i \lambda_{i^*} (\lambda_i y^2 + \lambda_i y_{i^*} + \lambda_{i^*} y - \lambda_i y^2 y_{i^*})}{\lambda^2 (1 + y y_i + y y_{i^*} - y - y^2)}. \quad (50)$$

*Proof.* Similar to the proof of Proposition 4, it is easy to show that  $p_{\mathbf{T}}(t^1, t^2) = 0$  if  $|t^1 - t^2| \neq -\Delta_d$ . For  $t > \Delta_d$ , consider regions 3 and 6,  $g_i(t) = \int_0^\infty [P_s(i)g_i(t+x) + P_s(i^*)g_i(t+x)] p_x dx$ . Hence,

$$g_i(t) = \lambda \int_0^\infty g_i(t+x) e^{-\lambda x} dx. \quad (51)$$

According to Lemma 3,  $g_i(t) \equiv 0$  for  $t > \Delta_d$ . Hence,  $p_{\mathbf{T}}(t^1, t^2) = 0$  if  $|t^1 - t^2| \neq -\Delta_d$  or  $t^1 + t^2 > \Delta_d$ .

For  $t \in (0, \Delta_d)$ , consider regions 3 and 4, (35) holds. Similar to the proof in Proposition 4 from (35) to (38), we conclude that  $\hat{g}_i = c_i e^{\lambda_{i^*} t}$  for some constant  $c_i$  such that

$$c_i = \lambda_{i^*} \hat{g}_i(0). \quad (52)$$

Then (48) is verified. We solve for  $c_i$  below.

Consider region 1. The point mass at 0 has the same expression as in the FIFO case,

$$\hat{g}_i(0) = \frac{\lambda_i}{\lambda} [\mathcal{I}_i + e^{-\lambda\Delta_d} \mathcal{I}_{i^*}]. \quad (53)$$

Consider region 5. The point mass at  $\Delta_d$  satisfies  $\hat{g}_i(\Delta_d) = \lambda_i \int_0^\infty \int_x^{\Delta_d} g_{i^*}(\tau) d\tau e^{-\lambda x} dx$ . By changing the order of integration, we have  $\hat{g}_i(\Delta_d) = \lambda_i \int_0^{\Delta_d} \int_0^\tau e^{-\lambda x} dx g_{i^*}(\tau) d\tau = \frac{\lambda_i}{\lambda} \int_0^{\Delta_d} (1 - e^{-\lambda\tau}) g_{i^*}(\tau) d\tau$ . Hence,

$$\hat{g}_i(\Delta_d) = \frac{\lambda_i}{\lambda} [\mathcal{M}_{i^*} - \mathcal{I}_{i^*}]. \quad (54)$$

Given the definition in (25),

$$\mathcal{M}_i = \hat{g}_i(0) + \frac{c_i}{\lambda_{i^*}} [e^{\lambda_{i^*} \Delta_d} - 1] + \hat{g}_i(\Delta_d), \quad (55)$$

$$\mathcal{I}_i = \hat{g}_i(0) + \frac{c_i}{\lambda_i} [1 - e^{-\lambda_i \Delta_d}] + \hat{g}_i(\Delta_d) e^{-\lambda_i \Delta_d}. \quad (56)$$

Moreover, the probability should add up to one,

$$\mathcal{M}_1 + \mathcal{M}_2 = 1. \quad (57)$$

Solving (52) to (57), we conclude that  $\mathcal{M}_i = \frac{\lambda_i}{\lambda}$  and  $c_i$  satisfies (50).  $\square$

**Corollary 8** (Steady State Vehicle Delay under FO). *The steady state vehicle delay under FO has the distribution*

$$P_d(t) = \frac{c_2}{\lambda_1} e^{\lambda_1 t} + \frac{c_1}{\lambda_2} e^{\lambda_2 t} + \frac{2\lambda_1 \lambda_2}{\lambda^2} (1 - e^{-\lambda t}) \quad (58)$$

$$+ \frac{c_2}{\lambda_2 y_1} (e^{-\lambda t} - e^{-\lambda_1 t}) + \frac{c_1}{\lambda_1 y_2} (e^{-\lambda t} - e^{-\lambda_2 t}),$$

with expected delay

$$E(d) = \frac{c_2}{\lambda_1} \mathcal{E}(\lambda_1) + \frac{c_1}{\lambda_2} \mathcal{E}(\lambda_2)$$

$$- \frac{c_2}{\lambda_2 y_1} \mathcal{E}(-\lambda_1) - \frac{c_1}{\lambda_1 y_2} \mathcal{E}(-\lambda_2)$$

$$+ \left( \frac{c_2}{\lambda_2 y_1} + \frac{c_1}{\lambda_1 y_2} - \frac{2\lambda_1 \lambda_2}{\lambda^2} \right) \mathcal{E}(-\lambda), \quad (59)$$

where  $\mathcal{E}(\cdot)$  follows (46).

*Proof.* By (11), the steady state distribution of delay satisfies  $p_d(t) = \sum_{i=1,2} P_s(i) \int_0^\infty [g_i(t+x) + g_{i^*}(t+x-\Delta_d) + g_{i^*}(x-t+\Delta_d)] p_x dx$ . Using the result from Proposition 7, the steady state distribution of the vehicle delay satisfies (58). It is easy to verify  $P_d(0) = \frac{c_2}{\lambda_1} + \frac{c_1}{\lambda_2} = \hat{g}_1(0) + \hat{g}_2(0)$  and  $P_d(\Delta_d) = 1$ . The expected mean  $E(d) = \int_0^{\Delta_d} t dP_d(t)$  satisfies (59).  $\square$

Corollary 8 implies that the distribution of vehicle delay in FO no longer equals the sum of traffic delay in all lanes. In FIFO, the two equal by Corollary 5.

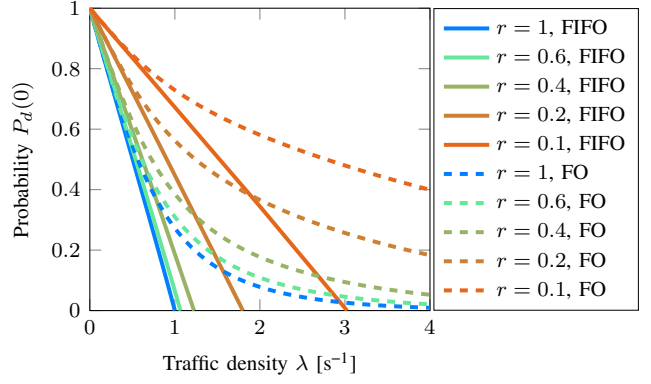
#### IV. ANALYSIS

This section discusses how delay is affected by traffic density  $\lambda$ , density ratio  $r := \lambda_1/\lambda_2$ , passing order (FIFO or FO), and temporal gap  $\Delta_d$ .  $\Delta_s = 0$  is assumed. In particular, we evaluate the probability of zero delay  $P_d(0) = \hat{g}_1(0) + \hat{g}_2(0)$  in Fig. 7, expected delay  $E(d)$  in Fig. 8, and steady state distribution of delay  $P_d(t)$  in Fig. 9. The curves are from direct analysis. Approximation (41) is used for FIFO. The accuracy of the analytical solutions is verified by EDS in Fig. 8c.

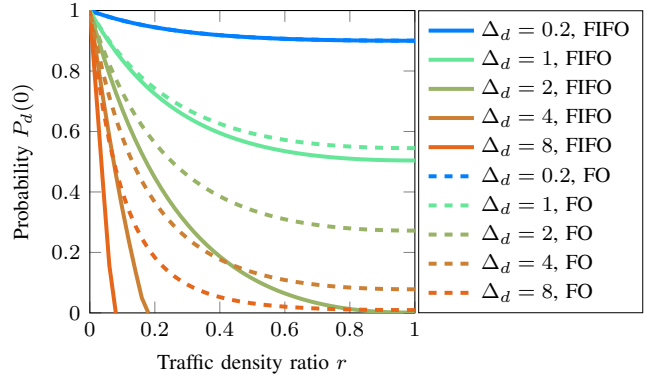
##### A. Delay and Traffic Density

In general, larger traffic density results in larger delay. According to Fig. 7a, the probability of zero delay  $P_d(0)$  drops when the traffic density goes up. In FIFO, it drops linearly and reaches zero when the equality in (21) holds, where

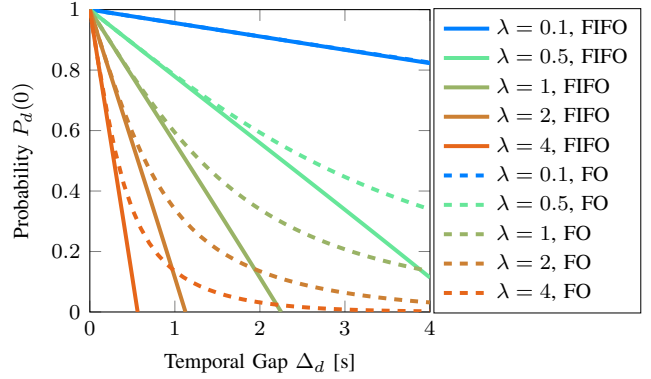
$$\lambda = \frac{(1+r)^2}{2\Delta_d r}. \quad (60)$$



(a) Fix  $\Delta_d = 2$  s.



(b) Fix  $\lambda = 1$  s<sup>-1</sup>.



(c) Fix  $r = 0.5$ .

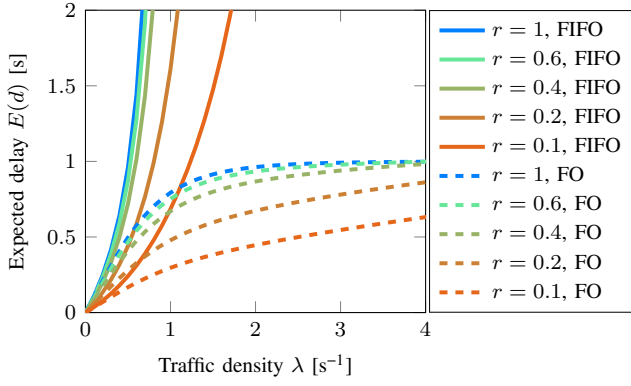
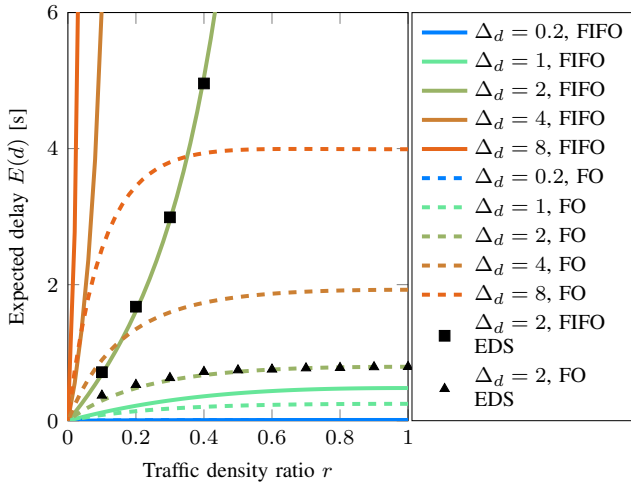
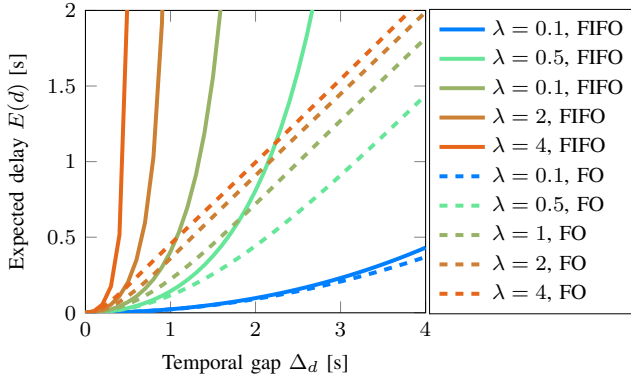
Fig. 7: The probability of zero delay  $P_d(0)$ .

In FO,  $P_d(0)$  drops with decreasing rate. According to Fig. 8a, the expected delay  $E(d)$  grows with the traffic density  $\lambda$ . In FIFO, it grows exponentially with  $\lambda$ , and goes to infinity when  $\lambda$  approaches (60). In FO, it grows with decreasing rate when  $\lambda$  increases. Fig. 9a illustrates the distribution of delay for  $\lambda \in \{0.1, 0.5, 1, 2, 4\}$ ,  $\Delta_d = 2$ , and  $r = 0.5$ . The distribution does not converge for  $\lambda > 1.125$  in FIFO, while it always converge in FO. It is easy to verify that the necessary condition (47) is always satisfied when  $\Delta_s = 0$ .

##### B. Delay and Density Ratio

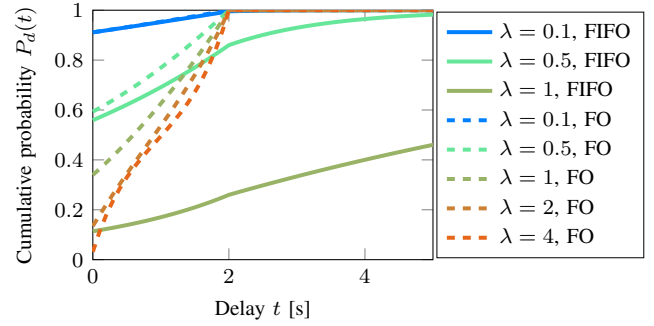
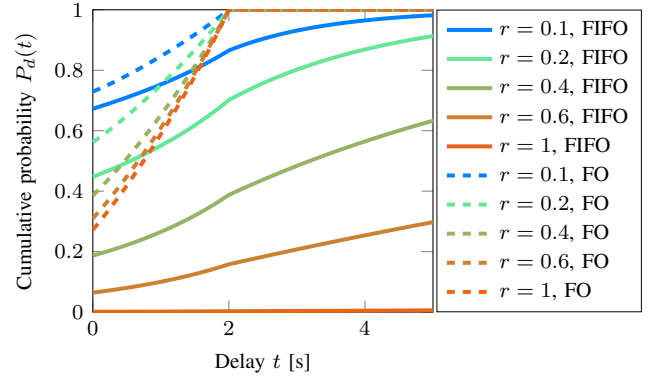
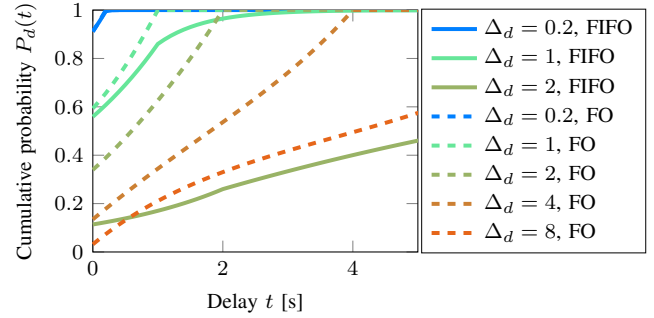
In general, there are more delays when the traffic is more balanced. According to Fig. 7b,  $P_d(0)$  drops with decreasing



(a) Fix  $\Delta_d = 2$  s.(b) Fix  $\lambda = 1$  s<sup>-1</sup>.(c) Fix  $r = 0.5$ .Fig. 8: The expected delay  $E(d)$ .

rate when the density ratio approaches 1. In FIFO, it reaches zero when (60) holds. In FO,  $P_d(0)$  is relatively constant for  $r > 0.5$ . According to Fig. 8b, the expected delay  $E(d)$  grows with respect to the density ratio  $r$ . In FIFO, the expected delay grows exponentially with  $r$  when there is a solution for  $r \leq 1$  in (60) for fixed  $\lambda$  and  $\Delta_d$ , e.g.,

$$\lambda \Delta_d \geq \min_{r \in (0,1]} \frac{(1+r)^2}{2r} = 2. \quad (61)$$

(a) Fix  $\Delta_d = 2$  s and  $r = 0.5$ .(b) Fix  $\Delta_d = 2$  s and  $\lambda = 1$  s<sup>-1</sup>.(c) Fix  $\lambda = 1$  s<sup>-1</sup> and  $r = 0.5$ .Fig. 9: Distribution of steady state vehicle delay  $P_d(t)$ .

The expected delay grows with decreasing rate when there is no solution for  $r \leq 1$  in (60), i.e.,  $\lambda \Delta_d < 2$ . In FO, the expected delay grows in decreasing rate when  $r$  approaches 1. When  $\lambda \Delta_d$  is small, the expected delay in FIFO is close to the expected delay in FO.

### C. Delay and Passing Order

For all scenarios in Fig. 7, Fig. 8, and Fig. 9, FO results in smaller delay than FIFO. The advantage of FO is due to the fact that the passing order is adaptable to real time scenarios. They have similar performances when either  $\lambda$ ,  $\Delta_d$ , or  $r$  is small. In those cases, the order determined by FO is close to the order in FIFO. Moreover, it is worth noting that the delay distribution in Fig. 9 is not computed for a single vehicle, but for all vehicles on average. Such average delay does not exceed  $\Delta_d$  in FO, but it is possible for individual vehicles

to have delay greater than  $\Delta_d$ . Though FO is efficient in the sense that it minimizes delay, it sacrifices fairness by not obeying the passing order determined by the desired passing time. As a consequence, certain vehicles may experience larger delay compared to that in the FIFO case. The tradeoff between fairness and efficiency in different policies will be studied in the future.

#### D. Delay and Temporal Gap

In general, a larger temporal gap results in larger delay. According to Fig. 7c,  $P_d(0)$  drops when the temporal gap  $\Delta_d$  increases. In FIFO, it drops linearly and reaches zero when the equality in (60) holds. In FO, it drops with decreasing rate. According to Fig. 8c, the expected delay  $E(d)$  grows with respect to the temporal gap  $\Delta_d$ . In FIFO, the expected delay grows exponentially. In FO, it eventually reaches a constant growth rate. The temporal gap is a design parameter in vehicle policies, which is affected by the uncertainty in perceptions. When there are larger uncertainties in perception, in order to stay safe, vehicles tend to maintain larger gaps to other vehicles. The trade-off between safety and efficiency under imperfect perception will be studied in the future.

#### V. CONCLUSION

This paper presented a new approach to perform delay analysis for unmanaged intersections in an event-driven stochastic model. The model considered the traffic delay at an intersection as an event-driven stochastic process, whose dynamics encoded equilibria resulted from microscopic multi-vehicle interactions. With the model, the distribution of delay can be obtained through either direct analysis or event-driven simulation. In particular, this paper performed detailed analyses for a two-lane intersection under two different classes of policies corresponding to two different passing orders. The convergence of the distribution of delay and the steady state delay were derived through direct analysis. The relationships between traffic delay and multiple factors such as traffic flow density, unevenness of traffic flows, temporal gaps between two consecutive vehicles, and the passing order were discussed. In the future, such analysis will be extended to more complex vehicle policies, more complex road topologies, multiple intersections, and heterogeneous traffic scenarios.

#### REFERENCES

- [1] T. V. Mathew, "Signalized intersection delay models," *Lecture notes in Traffic Engineering and Management*, 2014.

- [2] J. Xi, W. Li, S. Wang, and C. Wang, "An approach to an intersection traffic delay study based on shift-share analysis," *Information*, vol. 6, no. 2, pp. 246–257, 2015.
- [3] Y. Jiang, S. Li, and K. Q. Zhu, "Traffic delay studies at signalized intersections with global positioning system devices," *ITE Journal*, vol. 75, no. 8, pp. 30–39, 2005.
- [4] M. VanMiddlesworth, K. Dresner, and P. Stone, "Replacing the stop sign: Unmanaged intersection control for autonomous vehicles," in *International Joint Conference on Autonomous Agents and Multiagent Systems*, vol. 3, pp. 1413–1416, IFAAMS, 2008.
- [5] V. Savic, E. M. Schiller, and M. Papatriantafilou, "Distributed algorithm for collision avoidance at road intersections in the presence of communication failures," in *Intelligent Vehicles Symposium (IV)*, pp. 1005–1012, IEEE, 2017.
- [6] S. Azimi, G. Bhatia, R. Rajkumar, and P. Mudalige, "Reliable intersection protocols using vehicular networks," in *International Conference on Cyber-Physical Systems, ICCPS '13*, pp. 1–10, ACM, 2013.
- [7] C. Liu, C. W. Lin, S. Shiraishi, and M. Tomizuka, "Distributed conflict resolution for connected autonomous vehicles," *IEEE Transactions on Intelligent Vehicles*, vol. 3, no. 1, pp. 18–29, 2018.
- [8] P. Gora and I. Rüb, "Traffic models for self-driving connected cars," *Transportation Research Procedia*, vol. 14, pp. 2207 – 2216, 2016. Transport Research Arena TRA2016.
- [9] M. Treiber and A. Kesting, "An open-source microscopic traffic simulator," *IEEE Intelligent Transportation Systems Magazine*, vol. 2, no. 3, pp. 6–13, 2010.
- [10] J. Barceló, J. Casas, J. L. Ferrer, and D. García, *Modelling Advanced Transport Telematic Applications with Microscopic Simulators: The Case of AIMSUN2*, pp. 205–221. Springer, 1999.
- [11] M. Fellendorf and P. Vortisch, *Microscopic Traffic Flow Simulator VISSIM*, pp. 63–93. Springer, 2010.
- [12] S. P. Hoogendoorn and P. H. L. Bovy, "State-of-the-art of vehicular traffic flow modelling," *Proceedings of the Institution of Mechanical Engineers, Part I: Journal of Systems and Control Engineering*, vol. 215, no. 4, pp. 283–303, 2001.
- [13] R. Corthout, G. Flötteröd, F. Viti, and C. M. Tampère, "Non-unique flows in macroscopic first-order intersection models," *Transportation Research Part B: Methodological*, vol. 46, no. 3, pp. 343 – 359, 2012.
- [14] G. Flötteröd and J. Rohde, "Operational macroscopic modeling of complex urban road intersections," *Transportation Research Part B: Methodological*, vol. 45, no. 6, pp. 903 – 922, 2011.
- [15] C. Liu and M. J. Kochenderfer, "Analytically Modeling Unmanaged Intersections with Microscopic Vehicle Interactions," *arXiv:1804.04746*, Apr. 2018.
- [16] F. Alché, X. Qian, and A. de La Fortelle, "Time-optimal coordination of mobile robots along specified paths," in *International Conference on Intelligent Robots and Systems (IROS)*, pp. 5020–5026, IEEE, 2016.
- [17] X. Qian, F. Alché, J. Grégoire, and A. de La Fortelle, "Autonomous intersection management systems: criteria, implementation and evaluation," *IET Intelligent Transport Systems*, vol. 11, no. 3, pp. 182–189, 2017.
- [18] C. Gardiner, *Stochastic methods*, vol. 4. Springer, 2009.
- [19] W. Michiels and S.-I. Niculescu, *Spectral Properties of Linear Time-Delay Systems*, ch. 1, pp. 3–31. SIAM, 2007.